Direct quantification of the modulation of interaction between cell- or surface-bound LFA-1 and ICAM-1

Joana Vitte, Anne Pierres, Anne-Marie Benoliel, Pierre Bongrand

Direct quantification of the modulation of interaction between cell- or surface-bound LFA-1 and ICAM-1

Joana Vitte, Anne Pierres, Anne-Marie Benoliel, and Pierre Bongrand[1]

Laboratoire d'Immunologie, INSERM U600, CNRS FRE 2059, Univ. Mediterranée, Hôpital de Ste-Marguerite, Marseille, Cedex, France

Abstract: The functional activity of leukocyte integrins is highly regulated by several mechanisms related to intrinsic molecular properties and receptor interaction with the cell membrane. Here, we present a microkinetic study of the lymphocyte function-associated antigen-1-mediated interaction between flowing Jurkat cells and surface- or cell-bound intercellular adhesion molecule-1 (ICAM-1). We conclude that adhesion is initiated by the formation of a single bond with ~0.3 s^{-1} dissociation rate, and attachment is subsequently strengthened by the formation of additional bonds during the next 10 s; exposing cells to Mg^{2+} or Mn^{2+} resulted in up to a 16-fold increase of the binding frequency, in line with reported measurements performed on isolated molecules with surface plasmon resonance methodology; cell-bound ICAM-1 molecules were more efficient in mediating adhesion than Fc-ICAM-1, properly oriented and bound by surface-adsorbed protein A; and quantitative analysis of binding frequency suggested that adhesion efficiency was ten- to 100-fold lower than the maximum value allowed by previously determined association rates of soluble molecules. It is concluded that the presented methodology provides a simple and unique way of dissecting the initial step of cell adhesion and discriminating between affinity and avidity modulation of adhesion receptors. *J. Leukoc. Biol.* 76: 594–602; 2004.

Key Words: *laminar flow chamber · confocal microscopy · receptor topography · avidity · dissociation rate*

INTRODUCTION

Leukocyte β2 integrins, such as lymphocyte function-associated antigen-1 (LFA-1)/CD11aCD18, play a major role in many immunological processes such as antigen presentation [1], T cell-mediated cytotoxicity [2, 3], or leukocyte adhesion to endothelial cells before transmigration to peripheral tissues during inflammatory reactions [4]. All these functions require a tight control of cell adhesiveness to allow appropriate attachment and detachment [5]. Accordingly, the functional activity of LFA-1 on lymphocytes is tightly regulated: Although these molecules are inactive on resting cells [6], within seconds following proper stimulation, they may undergo a dramatic increase of their capacity to bind their ligands and particularly, the ubiquitous intercellular adhesion molecule-1 (ICAM-1)/CD54 receptor [7].

The functions of leukocyte integrins are regulated by multiple mechanisms, including modulation of intrinsic receptor activity through allosteric changes [8], control of receptor efficiency through so-called postreceptor events [9], and adaptation of receptor expression [10].

It is well established that LFA-1 may exhibit different activation states, resulting in a marked difference in affinity for its ligand: Early experiments suggested that the affinity constant might display a 200-fold increase from an "inactive" value of 10^4 M^{-1} [11]. Recent studies made on the interaction between mutant molecules and their ligands with surface plasmon resonance technology suggested the existence of at least three affinity states of the molecule with high, intermediate, and low affinity ranging between 10^3 and 10^7 M^{-1}. The dissociation rate ranged between 0.01 and 5 s^{-1}, and the association rate varied between 3000 and 100,000 $M^{-1}s^{-1}$ [8, 12–14]. Although cells can control LFA-1 affinity through inside-out signaling, allosteric changes were often induced with divalent cations such as Mg^{++} or Mn^{++} or so-called function-enhancing monoclonal antibodies (mAb), which were shown to stabilize high-affinity states. Indeed, affinity changes are associated with extensive molecular reorganization, resulting in marked variation of epitope expression [8].

Although the importance of these conformational changes is considered as fairly well understood, much evidence showed that the capacity of cells to bind ICAM-1-bearing cells or microparticles was not fully accounted for by intrinsic receptor properties. Differences are referred to as "avidity effects", which may be mediated by a variety of processes, such as receptor clustering [15, 16], displacement between the tip of microvilli and other regions of the cell membrane [17], receptor mobility [18], or the capacity to induce leukocyte spreading on ICAM-1-bearing surfaces [19]. The strength of anchoring to the cell membrane and underlying cytoskeleton might also play a role in the regulation of adhesion receptors [20]. It is commonly assumed that receptor avidity is correlated to the capacity to form multivalent bonds. Many reports demonstrated that treat-

[1] Correspondence: Laboratoire d'Immunologie, INSERM U600, CNRS FRE 2059, Univ. Mediterranée, Hôpital de Ste-Marguerite, 270 Bd de Ste-Marguerite, 13009 France. E-mail: bongrand@marseille.inserm.fr

Received February 9, 2004; revised May 28, 2004; accepted May 31, 2004; doi: 10.1189/jlb.0204077.

ing lymphoid cells with phorbol esters and/or low doses of the microfilament inhibitor cytochalasin D often increased surface clustering of β2 integrins as well as the lateral mobility of these molecules [9, 18].

Although it would be desirable to determine the respective influence of intrinsic and extrinsic phenomena on the functional activity of cell receptors such as LFA-1, experimental data remain insufficient to achieve this goal. The main difficulty is to obtain actually quantitative information about the interaction between cell-bound molecules.

Recent experimental progress yielded a new understanding of the relationship between conventional properties of soluble molecules, such as affinity or kinetic rates of bond formation, and the behavior of surface-attached receptors. Indeed, a major breakthrough was achieved by studying the interaction of bound receptors and ligands at the single molecule level with powerful technologies such as laminar flow chambers [21–23], atomic force microscopy [24], or biomembrane force probes [25, 26].

Thus, atomic force microscopy was used to study the rupture of single bonds formed between LFA-1 molecules expressed by a T cell hybridoma and adsorbed ICAM-1 molecules [27]. The authors subjected cells to variable disruptive forces. The rupture frequency of bonds subjected to a low force F (i.e., less than several tens of piconewtons) was, respectively, 4 exp(F/27.6) and 0.17 exp(F/19.7) for low- and high-affinity states. Frequencies are expressed in s^{-1} and forces in piconewtons. Note that this expression for the force dependence of bond rupture was suggested by Bell [28] and found to apply to many cell-adhesion receptors [29]. Note also that a more complex behavior was demonstrated when disruptive forces were varied over a wide range of magnitudes [26, 27]. A limitation of this approach is that the derivation of rupture frequencies from experimental values of unbinding forces requires some data interpretation [30]. Also, the frequency of bond formation remains difficult to estimate.

In the present report, we studied the effect of intrinsic and postreceptor modulation on the kinetics of bond formation between LFA-1-expressing cells and surfaces or cells bearing ICAM-1 ligand. Our method is conceptually very simple: Receptor-bearing cells were driven along ligand-coated surfaces by very low hydrodynamic forces of order of 1 pN in a laminar flow chamber operated at a low shear rate. Under these conditions, a single ligand-receptor bond could maintain a cell at rest during a detectable amount of time. The rate of bond formation and dissociation could thus be obtained in a straightforward way by monitoring the frequency and duration of cell arrests. This methodology yielded the first determination of the lifetime of bonds formed by selectins [21]. More recently, it revealed the dramatic influence of function-enhancing or -inhibiting mAb on the lifetime of bonds formed between collagen and β1 integrin receptors [31]. In the present work, we studied the interaction between LFA-1-bearing cells from the human T lymphocyte Jurkat line and ICAM-1 molecules, which were homogeneously adsorbed on polystyrene surfaces or expressed by monolayers of vascular endothelial cell ECV304 cells. The affinity and organization of Jurkat LFA-1 receptors were also manipulated with magnesium and manganese ions or cytochalasin D and phorbol myristate acetate (PMA).

It is concluded that cell-surface attachment is initiated by a single molecular interaction with a lifetime consistent with values obtained on soluble molecules, and this is followed within several seconds by strengthening events that are dependent on integrin-affinity state and molecular environment. It was thus possible to obtain quantitative information about the function of receptors expressed by living cells.

MATERIALS AND METHODS

Cells

Jurkat cells, a kind gift from Dr. Françoise Birg (INSERM U119, Marseille, France), were cultured in RPMI-1640 medium supplemented with 20 mM HEPES, 10% fetal calf serum (FCS), 2 mM L-glutamine, 50 U/ml penicillin, and 50 U/ml streptomycin. They exhibited homogeneous expression of CD11a and CD18, as a single peak was revealed with flow cytometry. However, they did not express CD11b or CD11c. They expressed very late antigen-4/CD29dCD49, a receptor for vascular cell adhesion molecule 1 (VCAM-1). Also, this line expressed CD3 but not CD2.

Cells from the ECV304 line (American Type Culture Collection, Manassas, VA, ref. CRL-1998) were grown until confluency in minimum essential medium 199 supplemented with 50 U/ml penicillin, 50 μg/ml streptomycin, 2 mM L-glutamine, and 10% FCS. Immunofluorescence revealed that these cells stably expressed ICAM-1 adhesion molecules, not VCAM-1 or E-selectin.

Reagents

Protein A from *Staphylococcus aureus* was supplied by Sigma Chemical Co. (St. Louis, MO, ref. P6031). The ICAM-1-Fc fusion protein (human) was supplied by R&D Systems (Abingdon, UK, Cat. #720-IC-050). Anti-CD11a, a function-blocking immunoglobulin G1 (IgG1) produced by clone 25.3, was supplied by Immunotech (Beckman-Coulter-Immunotech, Fullerton, CA, Cat. #IMO 157). Anti-ICAM-1/CD54, an IgG1 from clone 84H10, was supplied by Immunotech. Biotinylated anti-ICAM antibody was supplied by PharMingen (San Diego, CA, murine IgG1 κ from clone HA58).

All fluorescent antibodies used for flow cytometry were supplied by Coulter (Miami, FL).

Cytochalasin D, a microfilament inhibitor, and PMA, a standard protein kinase C activator, were provided by Sigma Chemical Co.

Surface coating

Polystyrene petri dishes (Becton Dickinson, San Jose, CA, 35 mm diameter) were broken manually to prepare ICAM-1-coated surfaces. All further treatments were performed under wet atmosphere. First, 50 μl protein A solution (20 μg/ml) was deposited and incubated 90 min at 37°C before extensive (10×) wash with 0.2% bovine serum albumin (Sigma Chemical Co.), which was then added at 50 μl of 2%, and plates were washed again after 90 min at 37°C. Finally, ICAM-1-Fc was added (50 μg/ml solution), and plates were incubated overnight at 4°C. In some cases, ICAM-1-Fc was replaced with anti-LFA-1 mAb.

Surface density of ICAM-1 on binding surfaces

ECV304

The surface density of ICAM-1/CD54 molecules was assayed by standard enzyme-linked immunosorbent assay: Briefly, plated ECV304 cells were treated with biotinylated anti-CD54 and then alkaline-phosphatase-conjugated streptavidin (Sigma Chemical Co., S2890). After a final wash, the amount of bound streptavidin was determined with an alkaline phosphatase detection kit (Sigma Chemical Co., MT1000). Cell number was determined by microscopical counting after trypsin detachment of plated cells. The average cell area was estimated at 200 μm^2 by microscopical examination.

Absolute calibration was achieved as follows: Protein A-coated wells were incubated with known, decreasing amounts of biotinylated anti-ICAM-1 and were then washed, and alkaline-phosphatase-streptavidin was added and

quantified. It was assumed that all anti-ICAM-1 antibodies were bound by surface-adsorbed protein A when dilution was sufficient.

This method was found sensitive enough to detect 10^9 enzyme-labeled molecules in a well. The average number of molecules per cell was 92,357 ± 47,141 (SD) after 16 separate determinations. The number of ICAM-1 molecules per cell was thus estimated at 460 molecules/μm^2.

ICAM-1-coated surfaces

ICAM-1-Fc fusion protein (50 μg) was labeled with an Alexa Fluor 488 labeling kit (Molecular Probes, Eugene, OR, Ref. 20181, supplied by Interchim, Montluçon, France) and deposited on protein A-coated surfaces as described above. They were then assayed for fluorescence with a Leica confocal laser-scanning microscopy (CLSM) with a laser-scanning microscope. Fluorescence calibration was performed as described previously [32] by examining a series of fluoresent protein dilutions prepared as 5 μl liquid sheets between a microscope slide and a 22 × 22 mm^2 coverslip. This method allowed satisfactory measurement of surface densities down to ~100 molecules/μm^2.

Under standard conditions, ICAM-1-Fc-coated surfaces expressed 1372 ± 152 (SD) molecules/μm^2 (15 separate determinations).

Adhesion measurement

Flow generation

Our methods were described extensively in previous papers [31, 33, 34], and only specific features will be recalled. Chambers were assembled by applying plastic surfaces bearing cell monolayers or adsorbed ICAM-1-Fc to a plexiglas block with a cavity of ~0.1 × 6 × 20 mm^3. Jurkat cells were suspended (300,000/ml) in a solution containing 129 mM NaCl, 5 mM KCl, 1 mM $CaCl_2$, 1 mM $MgCl_2$, 10 mM glucose, 20 mM, pH 7.2, HEPES buffer, and 0.2% by weight bovine albumin. Cell suspensions were driven into the chamber with an electric syringe holder. Under standard conditions, the wall shear rate G_w was 3.3 s^{-1}. This could be calculated with the standard formula: $G_w = 6Q/w\,h^2$ (1), where Q is the flow rate (cm^3/s), and w and h are the cavity width and height, respectively.

As previously emphasized [35], parameter h presented fairly important variations, and its experimental determination with a microscope was fairly tedious. Therefore, to achieve reproducible values of the flow rate, it was found most convenient to adapt the flow rate so that the average velocity U of sedimented cells would be close to 20 μm/s. This procedure is based on the empirical formula [36]: $U = 0.86 \times a \times G_w$ (2), where a is the average cell radius (this was 6.73 μm).

Cell monitoring

The flow chamber was set on the stage of an inverted microscope (CK40, Olympus, Japan) bearing a 20× objective. This was connected to a standard video camera (hyper HAD, Sony, Japan). The image of a selected microscope field (250 μm width) was recorded for a typical period of 10 min with a VHS-type recorder for delayed analysis.

The recorder output was connected to a PCVision+ digitizer (Imaging Technology, Bedford, MA) mounted on an IBM-compatible desk computer. This allowed real-time digitization of images with 8-bit accuracy, yielding 512 × 512 pixel images. With our settings, pixel size was 0.51 μm along cell trajectories. Custom-made software allowed to superimpose a cursor driven by the computer mouse on live images. Individual cell trajectories were thus recorded by following the front edge of moving cells with the cursor and recording time and position with a frequency of ~20 points per second. The motion of a given cells thus appeared as a sequence of periods of uniform displacements with a fairly uniform velocity of order of 20 μm/s and arrests with a wide range of duration from a fraction of a second to more than 10 s. Our procedure was extensively used in the laboratory for many years and was found to allow clear-cut detection of arrests lasting more than ~0.2 s. The total displacement of every cell was also recorded.

Data analysis

For each experimental condition, results obtained in a set of separate experiments were pooled to calculate the total number N of binding events and the sum L of displacements undergone by all monitored cells. The binding frequency P was then calculated as the ratio: $p = N/L$ (3).

This parameter was expressed in mm^{-1}. The statistical accuracy of determination of P was estimated by using known properties of Poisson distribution, yielding $N^{1/2}/L$ as an estimate of the standard deviation.

The number B(t) of cells remaining bound at time t after arrest is simply the number of arrests lasting t second(s) or more. It is well-known from elementary chemical kinetics that if arrests were mediated by the formation of single bonds with a dissociation rate k_{off}, and no additional bond was formed during the arrest period, B(t) would follow the simple law: $B(t) = B(0)\exp(-k_{off}\,t)$ (4).

Thus, plotting ln[B(t)] versus time would yield a straight line with a slope equal to $-k_{off}$. This may be called an unbinding plot. As previously shown, at least two different mechanisms might impose an upward concavity on the unbinding plot: Adhesion might be strengthened by the formation of additional interactions [37]; and bond formation might be a multiphasic process with initial occurrence of a transient intermediate state [33, 38, 39].

The average dissociation rate during the time interval (t_1, t_2) was derived from the total number N_1 of arrests lasting t_1 or more and the number N_2 of arrests lasting t_2 or more with the following formula [33]: $k = \ln(N_1/N_2)/(t_2-t_1)$ (5).

The statistical standard deviation for the determination of k may be calculated as: $SD_k = [(N_1-N_2)/N_2/N_1]^{1/2}/(t_2-t_1)$ (6).

The standard deviation estimates were used to assess the significance of differences of results obtained under different experimental conditions with Student's *t*-test.

Microscopic study of cell membrane receptor topography

Integrin labeling

One million Jurkat cells were centrifuged, and pellets were incubated in 100 μl RPMI medium supplemented with 1 g/l bovine albumin in ice bath and 10 μg fluorescein-labeled anti-CD11a. They were incubated 60 mn in an ice bath, then washed with cold medium, and fixed with 1% paraformaldehyde before microscopical examination.

ICAM-1 labeling

Cells from the ECV304 line were plated on circular glass slides (10 mm diameter), which were coated with 100 μl RPMI-1640 medium containing 1 g/l bovine albumin and 10 μg fluorescein-labeled anti-ICAM-1/CD54 antibody. They were then processed as Jurkat cells.

The distribution of surface-adsorbed ICAM-1 was studied with fluorescent ICAM-1-Fc, which was prepared as described above.

Microscopical examination

Labeled cells and surfaces were examined with a confocal laser fluorescence microscopy (Leica CLSM) using an Argon/Krypton laser and a 40× dry objective. Pixel size was thus 245 × 245 nm^2 with a vertical resolution of order of 700 nm. Typically, a given cell was represented as a series of about six 512 × 512 pixel images (8-bit depth) with 2 μm separation between sequential section planes. It was found convenient to set a detection photomultiplier at a moderate value of ~600 V so that the background level would be sufficiently low to avoid any confusion between random noise and fluorescence of volume elements containing a few labeled molecules.

The image histogram was obtained with custom-made software written in the laboratory.

RESULTS

Jurkat cells readily adhere to ICAM-1-coated surfaces under flow

When cells were driven along surfaces coated with ICAM-1, they displayed periods of fairly uniform motion, interspersed with arrests of widely varying duration, ranging between a few tenths of a second and more than 10 s.

To test the specificity of these binding events, ICAM-1 was replaced with murine IgG1: In a first set of experiments, the binding frequency fell from 0.430 ± 0.074 mm^{-1} (316 cells) to

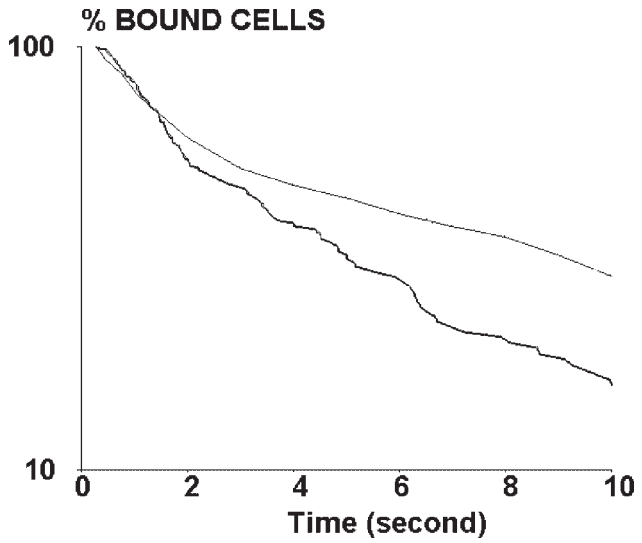

Fig. 1. Lifetime of LFA-1/ICAM-1 interaction. Jurkat cells were made to interact with ICAM-1-coated surfaces (thin line) or ICAM-1-bearing ECV304 cells (thick line), and the duration of arrests was recorded. The figure shows the rate of cell detachment.

0.099 ± 0.033 mm^{-1} (361 cells). Thus, most interactions between cells and ICAM-1-coated surfaces were specific.

Interaction between Jurkat cells and ICAM-1-coated surfaces involves at least two sequential phases

A total number of 2501 cells was monitored to determine the distribution of durations of binding events between Jurkat cells and ICAM-1-coated surfaces. As shown in **Figure 1**, the logarithm of the number of bound cells decreased linearly with respect to time during the first 2 s following arrest. This was consistent with the hypothesis of random rupture of attachments. As shown in **Table 1**, the rupture frequency was close to 0.3 s^{-1}. The detachment rate then decreased with a rupture frequency close to 0.1 s^{-1} during the time interval (2 s, 10 s). This was indicative of a bond-strengthening process. It was tempting to ascribe this strengthening to the formation of additional cell-surface bonds, as there was a strong negative correlation between adhesion frequency and detachment rate in this interval (5th and 7th columns of Table 1).

The frequency and duration of Jurkat binding to ICAM-1 are dramatically increased when LFA-1 affinity is increased

It has been shown repeatedly that leukocyte β2 integrins may shift toward higher affinity states by treatment with divalent cations such as magnesium or manganese. Thus, we studied the binding of Jurkat cells under different ionic conditions. Adhesion frequency exhibited a dramatic (16-fold) increase in the presence of 10 mM Mn^{++}. A tenfold increase was also obtained with a combination of $MgCl_2$ and EGTA. As shown in Table 1 under manganese or magnesium treatment, the initial detachment rate was close to control values, but detachment exhibited nearly a threefold decrease in the delayed phase [time interval (2 s, 10 s)]. It was tempting to ascribe these changes to an increase of the rate of bond formation between Jurkat LFA-1 and adsorbed ICAM-1.

It was often reported that LFA-1 activity could be enhanced by phorbol esters and/or cytochalasin D through postreceptor events such as increase of receptor mobility and/or integrin clustering. Therefore, we studied the effect of PMA (not shown) and a combination of PMA and cytochalasin D (Table 1) on the dynamic interaction between Jurkat cells and adsorbed ICAM-1. No detectable stimulation of adhesion frequency or duration was obtained.

Jurkat cells interact less efficiently with ICAM-1 than with anti-LFA-1 antibodies under standard conditions

It was found interesting to replace ICAM-1-Fc with anti-CD11a antibodies, which were expected to bind the same molecules on Jurkat cells (i.e., LFA-1) and on surfaces (i.e., protein A). This would allow direct comparison of binding-site function, as postreceptor effects should be similar in both systems. As shown in Table 1, the binding frequency measured on LFA-1 was more than fourfold higher than found on ICAM-1 ($P < 0.0001$). Also, the initial detachment rate was threefold lower with LFA-1 during the (0 s, 2 s) interval ($P < 0.0001$) and sixfold lower during the later (2 s, 10 s) interval.

As this higher efficiency of anti-LFA-1 might be a result of the twice-higher number of binding sites (IgG are divalent), we tried to assess the importance of binding-site density on adhesion efficiency: When coating ICAM-1 solution was diluted, resulting in more than a twofold decrease of ICAM-1 density, from 1372 to 620 molecules/μm^2, the adhesion frequency and

TABLE 1. Binding Jurkat Cells to Ligand-Coated Surfaces

Surface coating	Cell treatment	Cell number	Arrest number	Arrest frequency (mm^{-1})	Detachment rate (0 s, 2 s)	Detachment rate (2 s, 10 s)
ICAM-1	–	2501	274	0.445 ± 0.027	0.298 ± 0.027	0.094 ± 0.011
ICAM-1	$MgCl_2$/EGTA	100	90	4.26 ± 0.54	0.44 ± 0.067	0.040 ± 0.012
ICAM-1	$MnCl_2$	48	64	7.42 ± 1.36	0.302 ± 0.057	0.032 ± 0.012
ICAM-1	CytoD/PMA	1891	234	0.504 ± 0.034	0.338 ± 0.032	0.072 ± 0.010
anti-LFA-1	–	328	154	2.256 ± 0.220	0.112 ± 0.020	0.014 ± 0.004

Jurkat cells were driven along ICAM-1-coated surfaces in the presence of a wall shear rate of 3.3 s^{-1} for determination of the frequency and duration of binding events. Mean values are shown together with SE, which were calculated as explained in Materials and Methods. Standard conditions were altered with 5 mM $MgCl_2$ and 1 mM EGTA (2nd line) or 10 mM $MnCl_2$ (3rd line) or 5 μg/ml cytochalasin D and 100 ng/ml PMA (4th line).

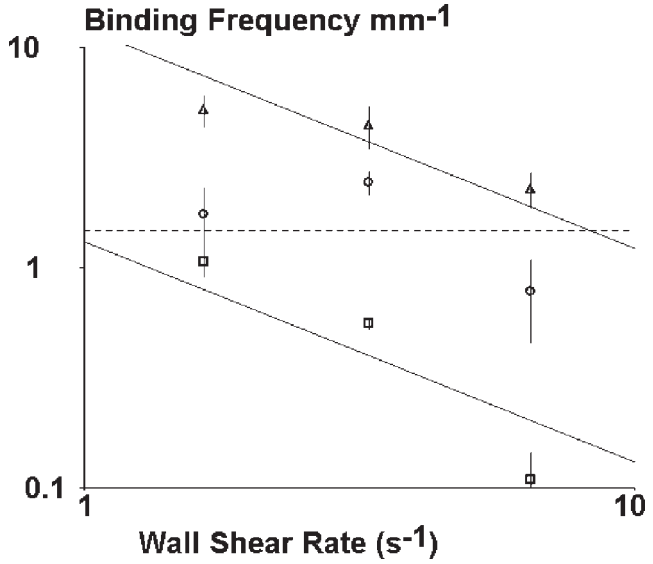

Fig. 2. Effect of the wall shear rate on adhesion efficiency. Jurkat cells were driven along ICAM-1-coated surfaces in low hydrodynamic flow with a wall shear rate ranging from 1.65 s^{-1} to 6.6 s^{-1}. The adhesion frequency was determined under control conditions (□) or after increasing LFA-1 affinity with 10 mM Mn^{++} (△). Vertical bar length is twice the calculated SE. Lines with a fixed slope of –1 were built by least square fit with experimental values. Interaction with anti-LFA-1-coated surfaces was also studied (○). As binding frequency was not significantly dependent on the shear rate, a line with a fixed slope of 0 was built by least square fit (broken line).

initial detachment rate were not significantly altered (not shown).

The kinetic association constant between LFA-1 and ICAM-1 is a limiting parameter for adhesion frequency

There are at least two possible ways of interpreting binding frequencies: First, ligand-receptor interaction may be rapid enough that each collision between a receptor and its ligand might result in bond formation. In this case, the binding frequency would represent the frequency of encounters between cell receptors and surface ligands. Thus, the binding frequency per millimeter displacement should be independent of cell velocity. Alternatively, ligand-receptor association might be too slow to allow each molecular encounter to result in bond formation. In this case, the binding frequency per millimeter should be inversely proportional to the cell velocity.

This was an incentive to study the effect of the wall shear rate on binding frequency: As shown in **Figure 2**, binding frequency per mm was markedly decreased when the wall shear rate exhibited a fourfold increase ($P<0.01$). Similar results were obtained when cells were exposed to manganese. It is interesting that the binding Jurkat to anti-LFA-1-coated surfaces was not significantly decreased (Student's $t=1.5$, $P>0.05$) when the wall shear rate exhibited a fourfold increase, from 1.65 s^{-1} to 6.6 s^{-1}.

Jurkat cells bind more readily to ICAM-1-bearing ECV304 cells than to adsorbed ICAM-1, but bond strengthening is decreased when ICAM-1 is born by cells rather than artificial surfaces

It is of obvious importance to understand the effect of surrounding membrane on the functional capacity of cell-surface receptors. Therefore, we studied the interaction between Jurkat and ECV304 cells, which were found to express ICAM-1 with a nearly threefold lower density than surfaces used in the first part of this study (i.e., 460 vs. 1372 molecules/μm^2). Results of adhesion experiments are shown in **Table 2**.

The first conclusion is that Jurkat LFA-1 readily interacted with ECV304 ICAM-1, as numerous arrests were recorded, and binding frequency was decreased twofold with a function-blocking anti-LFA-1 antibody. It is interesting that this treatment strongly increased the detachment rate in the second period of time (2 s, 10 s) in accordance with the hypothesis that this step should be dependent on the ease of bond formation.

Second, binding was enhanced by the cell membrane environment, as the binding frequency was more than twofold higher on cellular ICAM-1 than on adsorbed ICAM-1, although the ICAM-1 surface density was higher on the latter surface. It is interesting that the initial and delayed detachment rates were not significantly different.

Third, we studied the effect of LFA-1 manipulation on cell interaction with ICAM-1-expressing cells. As shown in Table 2, manganese significantly increased binding frequency ($P<0.01$) without any effect on detachment rates. A combination of cytochalasin D and PMA also increased binding frequency without any significant effect on detachment rates.

Distribution of adhesion receptors on interacting surfaces

As receptor clustering is thought to play an important role in adhesive efficiency, it was useful to study the distribution of LFA-1 and ICAM-1 molecules on interacting surfaces. This was done with confocal microscopy, and representative images are shown in **Figure 3**.

TABLE 2. Binding Jurkat Cells to ICAM-1-Expressing Cell Monolayers

Jurkat cell treatment	Number of counted cells	Arrest number	Arrest frequency (mm^{-1})	Detachment rate (0 s, 2 s)	Detachment rate (2 s, 10 s)
–	563	168	1.194 ± 0.092	0.317 ± 0.036	0.154 ± 0.021
MnCl2	382	166	1.738 ± 0.135	0.252 ± 0.027	0.158 ± 0.017
CytoD/PMA	301	171	2.272 ± 0.173	0.289 ± 0.109	0.109 ± 0.015
Anti-LFA-1	1001	149	0.595 ± 0.049	0.252 ± 0.033	0.263 ± 0.035

Jurkat cells were driven along ICAM-1-bearing ECV304 monolayers in the presence of a wall shear rate of 3.3 s^{-1} for determination of the frequency and duration of binding events. Mean values are shown together with SE, which were calculated as explained in Materials and Methods.

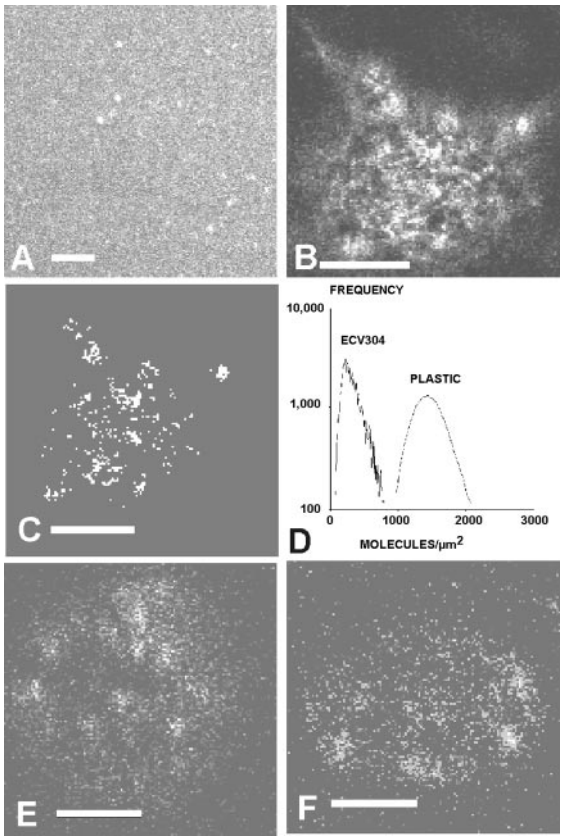

Fig. 3. Distribution of adhesion molecules on interacting surfaces. Confocal microscopy was used to study the distribution of (A) ICAM-1 on protein A-coated surfaces, (B) ICAM-1 on ECV304 cells, (E) LFA-1 on control Jurkat cells, and (F) LFA-1 on Jurkat cells treated with cytochalasin D and PMA. The section plane was fixed on the top of observed cells (B, E, and F). The pixels in (B) where the intensity is twice the average intensity or higher, are shown (C). The histograms of pixel brightness distribution for image (A, plastic; and B, ECV304) are displayed (D). Original bar, 10 μm.

First, surfaces coated with fluorescent ICAM-1 molecules were examined: As exemplified in Figure 3A, these surfaces displayed a low density of bright fluorescent aggregates (~0.01/μm^2, 0.1–1 μm^2 each), randomly scattered on a fairly regular background with fine-grained speckles. In contrast, ECV304 cells displayed more heterogeneous distribution of ICAM-1 molecules (Fig. 3B). To make this comparison more quantitative, the histograms of confocal images were studied. All studied cell histograms were fairly similar, and the fluorescence intensity distribution determined on ICAM-1-coated surfaces and ECV304 cells is shown in Figure 3D. Quantitative analysis of these data yielded the following conclusions: The average density of ICAM-1 on the representative cell shown in Figure 3B was 368 molecules/μm^2, as compared with the estimated value of 1372 molecules/μm^2 on ICAM-1-coated plastic; and the cell regions where the fluorescence was at least twice the mean value occupied ~4% of the total area and included ~11% of the total amount of labeled molecules. These regions are shown in Figure 3C. In contrast, the regions of ICAM-1-coated surfaces with at least twice the average intensity covered ~0.14% of the total surface and 0.4% of the total amount of fluorescence. Thus, fluorescence clustering is markedly higher on ECV304 cells than on ICAM-1-coated surfaces. Last, however, intensity distributions are clearly separated (Fig. 3D), and even on the brightest pixels of cell images, the average ICAM-1 density was lower than on ICAM-1-coated surfaces.

The distribution of LFA-1 molecules on Jurkat cells was also studied (Fig. 3, E and F): After examining several hundred cells, it was concluded that these integrins appeared as large clusters of a few micrometers in diameter. No significant difference could be found between the distribution of LFA-1 molecules on control cells and cells treated with PMA and/or cytochalasin D.

DISCUSSION

This work was aimed at relating the affinity and binding efficiency of the LFA-1 integrin. For this purpose, we used a laminar flow chamber operated at a low shear rate to monitor the initial attachment of flowing Jurkat cells to ICAM-1 molecules born by cells or artificial surfaces. The interest of using a low flow rate is twofold: First, this allowed sensitive dectection of single molecular bonds formed by low-affinity receptor-ligand couples such as CD2/CD48 [37] or even cadherins [34]. Second, as cell motion is slow enough to allow monitoring of all cells moving along the chamber floor before attachment, the rate of bond formation can be accurately measured. Our main results may be summarized as follows: Jurkat cells readily bound ICAM-1 molecules through a LFA-1-dependent mechanism; and under all tested conditions, the initial binding event displayed a fairly constant dissociation rate close to 0.3 s^{-1}. This transient attachment exhibited substantial time-dependent strengthening during the first 10 s following initial arrest. In addition, when Jurkat cells were exposed to an ionic environment known to increase LFA-1 affinity (i.e., $MnCl_2$ or $MgCl_2$+EGTA), the frequency of binding events was dramatically increased as well as the rate of attachment strengthening; and a quantitative study of the effect of cell velocity on binding frequency showed that this binding frequency reflected the efficiency of binding molecules rather than the rate of molecular encounters.

Thus, our study revealed quantitative features of the modulation of the integrin activation state that had not been obtained on cell-bound molecules with other methods. We shall now discuss the significance of these findings, which should help obtain a better understanding of the link between the affinity and avidity of cell adhesion receptors.

First, a major issue is to determine whether we actually detected single bonds. The strongest support to this hypothesis is probably the finding that under all experimental conditions, we detected an initial binding event with a consistent dissociation rate close to 0.3 s^{-1}. Indeed, an initial detachment rate was not altered on modification of the surface density of ICAM-1 (first rows of Tables 1 and 2) or LFA-1 availability (first and fourth rows of Table 2). However, if binding events were mediated by multiple bonds, changing receptor density should alter bond number and subsequently, bond duration. The only alternate possibility would be that the initial binding event might represent the minimum detectable bond number: In this case, LFA-1/ICAM-1 interaction should be much

shorter than several tenths of a second, which represents the sensitivity limitation of our experimental setup. However, as we shall now discuss, this possibility is unlikely, as bonds were subjected to minimal disruptive forces, suggesting that their duration is close to the lifetime of unstressed bonds; and reported values of LFA-1/ICAM-1 dissociation rates obtained with other methods consistently fell within the detection range of our apparatus. On the one hand, under our experimental conditions, bonds were subjected to minimal stress: A sphere of 6.7 μm radius bound to a plane and exposed to a flow of 3.3 s^{-1} shear rate experiences a disruptive force of ~1.4 piconewton [40]. If attachment is mediated by a single bond, the force experienced by this bond depends on the precise membrane shape in the contact area, but it is likely to be lower than ~10 piconewton [22, 39]. This is lower than the smallest unbinding force reported by Zhang and colleagues [27] when they studied the rupture of individual ICAM-1/LFA-1 bonds with atomic force microscopy. Conversely, the initial cell detachement rate we measured (i.e., ≈0.3 s^{-1}) was comparable with previous estimates of 0.12 s^{-1} for wild-type LFA-1 in the presence of 2 mM Mg^{++} [12, 13], as obtained with surface plasmon resonance technology. This is close to the low force dissociation frequency limit of 0.17 s^{-1} obtained by Zhang et al. [27] based on Bell's law [28]. Finally, this value is consistent with the dissociation rate measured on intermediate affinity mutants [8], which ranged between 0.43 and 0.76 s^{-1}.

A somewhat unexpected finding was that the initial detachment rate was not decreased in medium containing high magnesium or manganese concentration (Table 1, rows 1–3), and LFA-1 affinity should be increased under these conditions. Two explanations might be considered to account for this finding: First, LFA-1/ICAM-1 association might be a multistep event involving the formation of a transient complex with 0.3 s^{-1} dissociation rate and spontaneous strengthening later than 10 s after initial attachment. Such a delayed strengthening would be difficult to quantify with our methodology, and only this step would be enhanced by magnesium or manganese. Second, arrests observed in standard medium might be mediated by a low proportion of high-affinity LFA-1 molecules. To test this possibility, preliminary experiments were performed to block high-affinity LFA-1 by preincubating cells with 0.25 mg/ml soluble ICAM-1 for 20 min before adhesion tests: Although arrest frequency exhibited 96% inhibition by ICAM-1 in magnesium/EGTA medium (from 7.82±0.91 mm^{-1} to 0.45±0.12 mm^{-1}), no effect was observed in standard calcium/magnesium medium [arrest frequencies were, respectively, 0.38±0.07 mm^{-1} and 0.35±0.05 mm^{-1} after following 271 cells (32 arrests) in the absence of soluble ICAM-1 and 453 cells (49 arrests) with soluble ICAM-1]. Although these preliminary results would tend to support the multistep hypothesis, further studies are required to achieve definitive interpretation of our findings.

A major consequence of our capacity to detect single bonds is that our method provides a unique way of measuring the rate of bond formation between surface-attached adhesion receptors and ligands. Our finding that manganese activation resulted in a 16-fold increase of binding frequency is consistent with the recent report [8] of ~50-fold range of association constants measured on LFA-1 mutants locked in different states. This is also in line with a previous report [41] demonstrating a kinetic activation of CD11bCD18 integrin. Thus, it is reasonable to assume that binding frequency reflected the association rate of LFA-1 receptors.

This assumption is fully consistent with the remarkable negative correlation between arrest frequencies and delayed detachment rates [(2 s, 10 s) interval]: Indeed, a well-known mechanism for the upward concavity of detachment curves is the formation of additional bonds, as described with the master equation [21, 42]. It was therefore an expected finding that increased efficiency of bond formation resulted in concomitant increase of binding frequency and rate of attachment strengthening. It was also most significant that decreasing LFA-1 availability with a blocking antibody (Table 2, bottom row) reduced binding frequency and abolished bond strengthening.

However, the above interpretation of experimental data is not unique, and other possibilities should be considered.

First, it was previously demonstrated [43] that ICAM-1 could undergo spontaneous dimerization, thus enhancing LFA-1-mediated adhesion. Therefore, it would be a plausible hypothesis that the biphasic detachment curves we reported might represent the dissociation of a mixture of cells retained by monomer and dimer bonds. However, if this were the case, the early and late dissociation rates should be constant under all tested conditions. As shown in Figure 1, this is not the case, as the detachment rate measured in the (2 s, 10 s) period of time was higher on ECV304 cells, where ICAM-1 density was lower, than on ICAM-1-coated surfaces. However, it is likely that an ICAM-1 dimer bound to a single LFA-1 molecule should be a preferential binding site for an additional LFA-1 receptor, and this possibility is by no means inconsistent with our overall interpretation.

Second, biphasic detachment curves might be accounted for by a time- and/or shear-dependent strengthening of single bonds. This interpretation is made plausible by numerous previous reports about multiphasic association between ligands and receptors such as antigen and antibodies [38, 39]. However, as the dissociation rate remained fairly constant during the whole (0 s, 10 s) interval when additional bond formation was impaired (Table 2, bottom row), it is unlikely that such a strengthening might influence the detachment kinetics during the first 10 s following bond formation.

There is another problem raised by our results: Although divalent cations strongly increased the frequency of Jurkat attachment to ICAM-1-coated surfaces, the dissociation rate was not significantly altered. This may seem in contrast with previous work done with surface plasmon resonance, suggesting the possibility of high-affinity LFA-1/ICAM-1 interaction with a dissociation rate as low as 0.01 s^{-1}. An attractive explanation would be that transient LFA-1/ICAM-1 complexes might undergo delayed strengthening with slow kinetics, as suggested above. Indeed, it was previously argued that the flow chamber technology might essentially probe the external region of the energy/distance curve (or the energy landscape) of ligand/receptor complexes [33]. Thus, although increasing LFA-1 affinity was shown to increase association rate and decrease dissociation rate [8, 12–14], with up to 10,000-fold affinity increase, our method might reveal only increases of the association rate, if only strengthened states were stabilized by

divalent cations. However, it must be emphasized that the transient states we detected are certainly relevant to physiological situations, and the flow chamber methodology might yield quantitative parameters influencing receptor avidity, which is not a fully quantitative concept, rather than affinity, which is rigorously defined by thermodynamics.

There is another point of concern with our results: Although the uptake of Jurkat LFA-1 by adsorbed antibodies appeared as more efficient than ICAM-1 association on the basis of low dissociation rate (Table 1, bottom row) and shear-independence (Fig. 2), it may seem surprising that Jurkat binding efficiency was lower on anti-LFA-1 than on surfaces coated with similar amounts of ICAM-1 (Table 1). Although this finding cannot be quantitatively explained, we wish to emphasize that artifactually decreased binding frequencies are often found when the flow chamber is used to probe highly efficient ligand-receptor couples, with high association rate and low dissociation rate, resulting in definitive arrest of cells or particles as soon as they encounter the chamber floor. This is usually associated with a low number of flowing cells, and it is felt that these few cells could pass through the microscope field, because they were selected for reduced adhesiveness, or they were incompletely sedimented.

It would be of prominent interest to achieve a quantitative understanding of the relationship between binding frequency and intrinsic molecular association rate. Indeed, this would help in obtaining a quantitative account of avidity. As previously discussed [44], it is very difficult to relate association constants between ligand-receptor couples in soluble versus surface-bound form. This difficulty may be illustrated by the following discussion: If we assume surface-adsorbed ICAM-1 molecules are fairly flexible structures, we may consider binding sites as confined in a planar slice of 20 nm thickness, corresponding to the length of molecules. Note that Dustin and colleagues [45] previously used the concept of confinement region with this order of magnitude. As the surface concentration was 1372 molecules/μm^2, the volume concentration was 68,600 molecules/μm^3, i.e., 1.1 10^{-4} M. As the binding frequency was $\sim$0.009 s^{-1} (corresponding to the binding frequency of 0.445 mm^{-1} shown in Table 1 and average velocity of 20 μm/s), we might estimate an upper value of the association rate by assuming that cell-surface contact is mediated by the tip of microvilli, with only one available LFA-1 molecule on this tip: The binding frequency would be $k_{on} \times 1.1\ 10^{-4}$ M, yielding an estimate of 82 $M^{-1}s^{-1}$ for k_{on} under control conditions and 1300 $M^{-1}s^{-1}$ after manganese activation. These estimates are ten- to 100-fold lower than values obtained on isolated molecules with surface plasmon resonance [12, 13]. This means that binding efficiency is limited by different parameters such as receptor availability on contact surfaces, flexibility, and possibly repulsion between cells and surfaces.

The importance of receptor availability is consistent with the finding that Jurkat cells adhered more readily on cell-bound ICAM-1 than on surface-adsorbed molecules, as binding frequency was 2.7-fold higher on ECV304 (compare Tables 1 and 2), and the ICAM-1 surface density was threefold lower (see Materials and Methods). This finding is an incentive to further study the mechanisms allowing cells to optimize the efficiency of adhesion receptors, possibly by ensuring optimal topographical distribution. It was tempting to relate this finding to ligand clustering. Indeed, confocal microscopy was often used to detect integrin clustering, and this clustering was frequently correlated to receptor activation [9]. However, although quantitative study of microscopical images revealed definite clustering of ICAM-1 molecules on ECV304 cells, it was impossible to relate these findings to functional data: Indeed, even in clustered areas, the average surface density per 0.06 μm^2 pixel of ICAM-1 on ECV304 cells was much lower than the average density on artificial ICAM-1-coated surfaces. Therefore, it must be concluded that topographical features detectable with standard resolution of confocal microscopy do not account for the high-binding efficiency of cell-bound ICAM-1.

Cytochalasin D and PMA had no significant effect on the interaction between Jurkat and adsorbed ICAM-1 (Table 1), and adhesion to cell-bound ICAM-1 was only weakly increased (Table 2). A possible interpretation would be that LFA-1 was fairly clustered in untreated Jurkat cells (Fig. 3E), in line with the finding that efficient adhesion was found in the absence of stimuli known to enhance avidity. This is also consistent with a previous report that "clustered" LFA-1 appeared as speckles of 0.8 μm^2 or more on images obtained with confocal microscopy [7]. It would certainly be warranted to apply our methodology to other cellular models to assess the significance of these findings.

In conclusion, we presented a microkinetic study of the modulation of intrinsic LFA-1 activity on a cellular model. This allowed a quantitative assessment of the modification of affinity states that were previously measured on isolated molecules with surface plasmon resonance. The main conclusions are that the initial binding event between LFA-1- and ICAM-1-coated surfaces is the formation of a short-lived complex with a dissociation rate of 0.3 s^{-1}; an important component of integrin function enhancement by divalent cations is an increase of the rate of bond formation; and incomplete molecular accessibility is a limiting parameter for association between surface-bound molecules, independently of affinity parameters. Thus, the binding frequency determined under our experimental conditions is an important determinant of avidity. Our approach provides a powerful tool to dissect the initial steps of cell adhesion and discriminate between affinity and avidity effects.

ACKNOWLEDGMENT

The authors are grateful to the section editor for suggesting blocking experiments with soluble ICAM-1.

REFERENCES

1. Grakoui, A., Bromley, S. K., Sumen, C., Davis, M. M., Shaw, A. S., Allen, P. M., Dustin, M. L. (1999) The immunological synapse: a molecular machine controlling T cell activation. *Science* **285,** 221–227.
2. Davignon, D., Martz, E., Reynolds, T., Kurzinger, K., Springer, T. A. (1981) Lymphocyte function-associated antigen 1 (LFA-1): a surface antigen distinct from Lyt-2,3 that participates in T lymphocyte-mediated killing. *Proc. Natl. Acad. Sci. USA* **78,** 4535–4539.

3. Bongrand, P., Pierres, M., Golstein, P. (1983) T cell-mediated cytolysis: on the strength of effector-target cell interaction. *Eur. J. Immunol.* **13,** 424–429.
4. Lawrence, M. B., Springer, T. A. (1991) Leukocytes roll on a selectin at physiologic flow rates: distinction from and prerequisite for adhesion through integrins. *Cell* **65,** 859–873.
5. Palecek, S. P., Loftus, J. C., Ginsberg, M. H., Lauffenburger, D. A., Horwitz, A. F. (1997) Integrin-ligand binding properties govern cell migration speed through cell-substratum adhesiveness. *Nature* **385,** 537–539.
6. Lub, M., van Vliet, S. J., Oomen, S. P. M. A., Pieters, R. A., Robinson, M., Figdor, C. G., van Kooyk, Y. (1997) Cytoplasmic tails of β 1, β 2 and β 7 integrins differentially regulate LFA-1 function in K562 cells. *Mol. Biol. Cell* **8,** 719–728.
7. Constantin, G., Majeed, M., Giagulli, C., Piccio, L., Kim, J. Y., Butcher, E. C., Laudanna, C. (2000) Chemokines trigger immediate β 2 integrin affinity and mobility changes: differential regulation and roles in lymphocyte arrest under flow. *Immunity* **13,** 759–769.
8. Shimaoka, M., Xiao, T., Liu, J. H., Yang, Y., Dong, Y., Jun, C. D., McCormack, A., Zhang, R., Joachimiak, A., Takagi, J., Wang, J. h., Spring, T. A. (2003) Structures of the αL I domain and its complex with ICAM-1 reveal a shape-shifting pathway for integrin regulation. *Cell* **112,** 99–111.
9. van Kooyk, Y., Figdor, C. G. (2000) Avidity regulation of integrins: the driving force in leukocyte adhesion. *Curr. Opin. Cell Biol.* **12,** 542–547.
10. Burns, A. R., Doerschuk, C. M. (1994) Quantitation of L-selectin and CD18 expression on rabbit neutrophils during CD18-independent and CD18-dependent emigration in the lung. *J. Immunol.* **153,** 3177–3188.
11. Lollo, B. A., Chan, K. W. H., Hanson, E. M., Moy, V. T., Brian, A. A. (1993) Direct evidence for two affinity states for lymphocyte-function-associated antigen 1 on activated T cells. *J. Biol. Chem.* **15,** 21693–21700.
12. Tominaga, Y., Kita, Y., Satoh, A., Asai, S., Kato, K., Ishikawa, K., Horiuchi, T., Takashi, T. (1998) Affinity and kinetic analysis of the molecular interaction of ICAM-1 and leucocyte function-associated antigen-1. *J. Immunol.* **161,** 4016–4022.
13. Lupher, M. L., Harris, E. A. S., Beals, C. R., Sui, L. M., Liddington, R. C., Staunton, D. E. (2001) Cellular activation of leukocyte function-associated antigen-1 and its affinity are regulated at the I domain allosteric site. *J. Immunol.* **167,** 1431–1439.
14. Shimaoka, M., Lu, C., Palframan, R. T., vonAndrian, U. H., McCormack, A., Takagi, J., Springer, T. A. (2001) Reversibly locking a protein fold in an active conformation with a disulfide bond: integrin αL I domains with high affinity and antagonist activity in vivo. *Proc. Natl. Acad. Sci. USA* **98,** 6009–6014.
15. van Kooyk, Y., Weder, P., Heije, K., Figdor, C. J. (1994) Extracellular Ca2+ modulates leukocyte function-associated antigen-1 cell surface distribution on T lymphocytes and consequently affects cell adhesion. *J. Cell Biol.* **124,** 1061–1070.
16. Stewart, M. P., McDowall, A., Hogg, N. (1998) LFA-1-mediated adhesion is regulated by cytoskeletal restraint and by a Ca2+-dependent protease, calpain. *J. Cell Biol.* **140,** 699–707.
17. Erlandsen, S. L., Hasslen, S. R., Nelson, R. D. (1993) Detection and spatial distribution of the α2-integrin (Mac-1) and L-selectin (LECAM-1) adherence receptors on human neutrophils by high-resolution field emission SEM. *J. Histochem. Cytochem.* **41,** 327–333.
18. Kucik, D. F., Dustin, M. L., Miller, J. M., Brown, E. J. (1996) Adhesion-activating phorbol ester increases the mobility of leukocyte integrin LFA-1 in cultured lymphocytes. *J. Clin. Invest.* **97,** 2139–2144.
19. Stewart, M. P., Cabanas, C., Hogg, N. (1996) T cell adhesion to intercellular adhesion molecule-1 (ICAM-1) is controlled by cell spreading and the activation of integrin LFA-1. *J. Immunol.* **156,** 1810–1817.
20. Dwir, O., Kansas, G. S., Alon, R. (2001) Cytoplasmic anchorage of L-selectin controls leukocyte capture and rolling by increasing the mechanical stability of the selectin tether. *J. Cell Biol.* **155,** 145–156.
21. Kaplanski, G., Farnarier, C., Tissot, O., Pierres, A., Benoliel, A-M., Alessi, M-C., Kaplanski, S., Bongrand, P. (1993) Granulocyte-endothelium initial adhesion. Analysis of transient binding events mediated by E-selectin in a laminar shear flow. *Biophys. J.* **64,** 1922–1933.
22. Alon, R., Hammer, D. A., Springer, T. A. (1995) Lifetime of P-selectin-carbohydrate bond and its response to tensile force in hydrodynamic flow. *Nature* **374,** 539–542.
23. Smith, M. J., Berg, E. L., Lawrence, M. B. (1999) A direct comparison of selectin-mediated transient, adhesive events using high temporal resolution. *Biophys. J.* **77,** 3371–3383.
24. Florin, E. L., Moy, V. T., Gaub, H. E. (1994) Adhesion forces between individual ligand-receptor pairs. *Science* **264,** 415–417.
25. Evans, E., Berk, D., Leung, A. (1991) Detachment of agglutinin-bonded red blood cells. I–Forces to rupture molecular-point attachments. *Biophys. J.* **59,** 838–848.
26. Merkel, R., Nassoy, P., Leung, A., Ritchie, K., Evans, E. (1999) Energy landscapes of receptor-ligand bonds explored with dynamic force spectroscopy. *Nature* **397,** 50–53.
27. Zhang, X., Vojcikiewicz, E., Moy, V. T. (2002) Force spectroscopy of the leukocyte function associated 1/intercellular adhesion molecule 1 interaction. *Biophys. J.* **83,** 2270–2279.
28. Bell, G. I. (1978) Models for the specific adhesion of cells to cells. *Science* **200,** 618–627.
29. Chen, S., Springer, T. A. (2001) Selectin receptor-ligand bonds: formation limited by shear rate and dissociation governed by the Bell model. *Proc. Natl. Acad. Sci. USA* **98,** 950–955.
30. Evans, E. (2001) Probing the relation between force-lifetime and chemistry in single molecular bonds. *Annu. Rev. Biophys. Biomol. Struct.* **30,** 105–128.
31. Masson-Gadais, B., Pierres, A., Benoliel, A. M., Bongrand, P., Lissitzky, J. C. (1999) Integrin α and β subunit contribution to the kinetic properties of α 2-β 1 collagen receptors on human keratinocytes analyzed under hydrodynamic conditions. *J. Cell Sci.* **112,** 2335–2345.
32. Pierres, A., Tissot, O., Malissen, B., Bongrand, P. (1994) Dynamic adhesion of CD8-positive cells to antibody-coated surfaces: the initial step is independent of microfilaments and intracellular domains of cell-binding molecules. *J. Cell Biol.* **125,** 945–953.
33. Pierres, A., Touchard, D., Benoliel, A. M., Bongrand, P. (2002) Dissecting streptavidin-biotin interaction with a laminar flow chamber. *Biophys. J.* **82,** 3214–3223.
34. Perret, E., Benoliel, A. M., Nassoy, P., Pierres, A., Delmas, V., Thiéry, J. P., Bongrand, P., Feracci, H. (2002) Fast dissociation kinetics of the recognition between individual E-cadherin fragments revealed by flow chamber analysis. *EMBO J.* **21,** 2537–2546.
35. Pierres, A., Feracci, H., Delmas, V., Benoliel, A. M., Thiéry, J. P., Bongrand, P. (1998) Experimental study of the interaction range and association rate of surface-attached cadherin 11. *Proc. Natl. Acad. Sci. USA* **95,** 9256–9261.
36. Tissot, O., Pierres, A., Foa, C., Delaage, M., Bongrand, P. (1992) Motion of cells sedimenting on a solid surface in a laminar shear flow. *Biophys. J.* **61,** 204–215.
37. Pierres, A., Benoliel, A. M., Bongrand, P., van der Merwe, P. A. (1996) Determination of the lifetime and force dependence of interactions of single bonds between surface-attached CD2 and CD48 adhesion molecules. *Proc. Natl. Acad. Sci. USA* **93,** 15114–15118.
38. Foote, J., Milstein, C. (1994) Conformational isomerism and the diversity of antibodies. *Proc. Natl. Acad. Sci. USA* **91,** 10370–10374.
39. Pierres, A., Benoliel, A. M., Bongrand, P. (1995) Measuring the lifetime of bonds made between surface-linked molecules. *J. Biol. Chem.* **270,** 26586–26592.
40. Goldman, A. J., Cox, R. G., Brenner, H. (1967) Slow viscous motion of a sphere parallel to a plane wall. II–Couette flow. *Chem Eng. Sci.* **22,** 653–660.
41. Cai, T. Q., Wright, S. D. (1995) Energetics of leukocyte integrin activation. *J. Biol. Chem.* **270,** 14358–14365.
42. Cozens-Roberts, C., Lauffenburger, D. A., Quinn, J. A. (1990) Receptor-mediated cell attachment and detachment kinetics. I. Probabilistic model and analysis. *Biophys. J.* **58,** 841–856.
43. Miller, J., Knorr, M., Ferrone, M., Houdei, R., Carron, C. P., Dustin, M. L. (1995) Intercellular adhesion molecule-1 dimerization and its consequences for adhesion mediated by lymphocyte function associated-1. *J. Exp. Med.* **182,** 1231–1241.
44. Pierres, A., Benoliel, A. M., Zhu, C., Bongrand, P. (2001) Diffusion of microspheres in shear flow near a wall: use to measure binding rates between attached molecules. *Biophys. J.* **81,** 25–42.
45. Dustin, M. L., Ferguson, L. M., Chan, P-Y., Springer, T. A., Golan, D. E. (1996) Visualization of CD2 interaction with LFA-3 and determination of the two-dimensional dissociation constant for adhesion receptors in a contact area. *J. Cell Biol.* **132,** 465–474.